EXPLICIT ALGEBRAIC SUBGRID-SCALE MODELS FOR LES

A. Rasam[1], *G. Brethouwer*[1] *and A.V. Johansson*[1]

[1] *Linné FLOW Centre, KTH Mechanics, SE-10044, Stockholm, Sweden*
rasam@mech.kth.se

Abstract

The explicit algebraic subgrid stress model (EASSM) has been introduced recently by Marstorp *et al.* (2009). The EASSM improves the prediction of the individual subgrid-scale (SGS) stresses and gives large-eddy simulation (LES) predictions that are less resolution dependent in comparison with isotropic eddy viscosity SGS stress models (Rasam *et al.* 2011). In the first part of the paper, we present LES results of turbulent channel flow at $Re_\tau = 934$ and 2003 using the EASSM and compare its performance to that of the dynamic Smagorinsky model (DSM) of Germano *et al.* (1991). We show that the EASSM predictions are much less resolution dependent and more accurate than those of the DSM at both Reynolds numbers.

In the second part of the paper, we present a new explicit algebraic subgrid scalar flux model (EASSFM) for LES of passive scalar transport. The new model is derived from the explicit algebraic scalar flux model of Wikström *et al.* (2000) for Reynolds averaged Navier–Stokes equations. The new model is derived from the modeled transport equation of the SGS scalar flux and has a tensorial eddy diffusivity formulation which uses the strain rate, rotation rate and the subgrid stress tensors in its formulation . The new model predictions of the SGS scalar fluxes are not necessarily aligned with the resolved scalar gradient. Therefore, it can predict SGS fluxes arising from the mean shear. The EASSFM is validated for the case of heat transfer in streamwise rotating turbulent channel flow (with Prandtl number $Pr = 0.71$ and friction Reynolds number $Re_\tau = 300$).

1 Introduction

Explicit algebraic models have been developed for the Reynolds averaged equations both for the stresses (Wallin and Johansson 2000) and scalar fluxes (Wikström *et al.* 2000). Their algebraic form is obtained via the use of a weak equilibrium assumption (Rodi 1976). They model the effect of shear on the anisotropy of the Reynolds stresses and the scalar fluxes better than the eddy viscosity and eddy diffusivity models, respectively, while their computational cost is comparable.

Marstorp *et al.* (2009) derived an explicit algebraic subgrid stress model (EASSM) for large-eddy simulation (LES), from the corresponding Reynolds stress model. Their derivation results in a nonlinear mixed model which improves the description of the SGS anisotropy in comparison with the isotropic eddy viscosity models. The better description of the SGS anisotropy by the EASSM leads to LES predictions that are less sensitive to the grid resolution. Rasam *et al.* (2011) showed that comparable LES predictions of mean velocity and Reynolds stresses can be obtained using the EASSM at a much lower computational cost than the isotropic eddy viscosity models.

The eddy diffusivity model (EDM) is often used in LES of passive scalar transport, since it is computationally inexpensive, but it has several known drawbacks arising from its simple formulation (Sagaut 2010). One is its inability to correctly predict the anisotropy of the mean scalar variance SGS dissipation (Kang & Meneveau 2001). The other is its deficiency in prediction of the SGS scalar fluxes arising from the mean shear. In this paper, we derive an explicit algebraic subgrid scalar flux model (EASSFM) for the passive scalar based on the explicit algebraic scalar flux model of Wikström *et al.* (2000) for the Reynolds averaged equations. The new model improves LES predictions over the DEDM and is validated in the case of turbulent channel flow with streamwise system rotation.

2 Numerical approach

Simulations are carried out using a pseudo-spectral Navier–Stokes solver. The code uses Fourier representation in wall-parallel directions and Chebychev representation in the wall-normal direction. The time integration is carried out using a third-order Runge–Kutta scheme for the nonlinear terms and a second-order Crank–Nicholson scheme for the linear terms (Chevalier *et al.* 2007).

3 Part I: Performance comparison of the EASSM and the DSM

We compare the performance of the EASSM in predicting the mean velocity and Reynolds stress profiles with that of the dynamic Smagorinsky model (DSM) of Germano *et al.* (1991). LESs of turbulent channel flow are carried out with a constant mass flux constraint at $Re_\tau = 934$ and 2003 at various resolutions, see table 1. The results are also compared to the DNSs by Hoyas and Jiménez (2008).

Explicit algebraic subgrid stress model (EASSM)

The EASSM has the following formulation for the

Case	Re_τ		Δx^+		Δz^+		N_y
	EASSM	DSM	EASSM	DSM	EASSM	DSM	
1	938.7	828.7	184.3	162.7	92.2	81.4	97
2	951.0	873.5	124.6	114.3	62.3	57.2	97
3	966.7	896.5	94.9	88.0	47.4	44.0	129
4	946.3	912.8	74.3	71.7	27.9	26.9	129
5	2012	1786	197.5	175.3	98.8	87.7	193
6	2031	1876	133.0	122.8	66.5	61.4	257
7	2070	1920	101.6	94.2	50.8	47.1	257
8	2031	1958	79.8	76.9	30.5	28.8	257

Table 1: Summary of the simulations. Δx^+ and Δz^+ are streamwise and spanwise resolutions in wall units in physical space, respectively. The number of points in the wall-normal direction is N_y.

SGS stress tensor

$$\tau_{ij}=K^{\text{SGS}}\left[\frac{2}{3}\delta_{ij}+\beta_1\tau^*\widetilde{S}_{ij}+\beta_4\tau^{*2}(\widetilde{S}_{ik}\widetilde{\Omega}_{kj}-\widetilde{\Omega}_{ik}\widetilde{S}_{kj})\right]. \quad (1)$$

The first term is the isotropic part, the second term is an eddy viscosity part and the third term is a nonlinear tensor that creates anisotropy of the SGS stresses. $\widetilde{S}_{ij}$ and $\widetilde{\Omega}_{ij}$ are the resolved strain rate and rotation-rate tensors. β_1 and β_4 determine the relative contribution of the eddy viscosity and the nonlinear terms and are given by

$$\beta_4 = -\frac{33}{20}\frac{1}{\left[(9c_1/4)^2+\tau^{*2}|\widetilde{\Omega}_{ij}|^2\right]},\ \beta_1=\frac{9}{4}c_1\beta_4, \quad (2)$$

where τ^* is the time scale of the SGS motions and $|\widetilde{\Omega}_{ij}|=\sqrt{2\widetilde{\Omega}_{ij}\widetilde{\Omega}_{ij}}$. The EASSM employed here models K^{SGS} as

$$K^{\text{SGS}}=c\,\Delta^2|\widetilde{S}_{ij}|^2 \quad |\widetilde{S}_{ij}|=\sqrt{2\widetilde{S}_{ij}\widetilde{S}_{ij}}, \quad (3)$$

where c is dynamically determined using the Germano identity with averaging in the homogeneous directions. The model parameter c_1 in equation (2) is determined from the dynamic coefficient c as

$$c_1=c_1'\sqrt{c_3'}\frac{c^{1.1}}{(2C_s)^{2.5}},\ c_1'=4.2,\ c_3'=2.4,\ C=1.6.$$

The SGS time scale, τ^*, is modeled as

$$\tau^*=c_3'\frac{1.5C^{1.5}\sqrt{c}}{2C_s}|\widetilde{S}_{ij}|^{-1},\ C_s=0.1. \quad (4)$$

System rotation is accounted for by replacing $\widetilde{\Omega}_{ij}$ in (1) and (2) by $\widetilde{\Omega}^R_{ij}$

$$\widetilde{\Omega}^R_{ij}=\widetilde{\Omega}_{ij}+\left(\frac{13}{4}\right)\epsilon_{ikj}\Omega_k, \quad (5)$$

where ϵ_{ijk} is the alternating tensor and Ω_k is the system rotation vector.

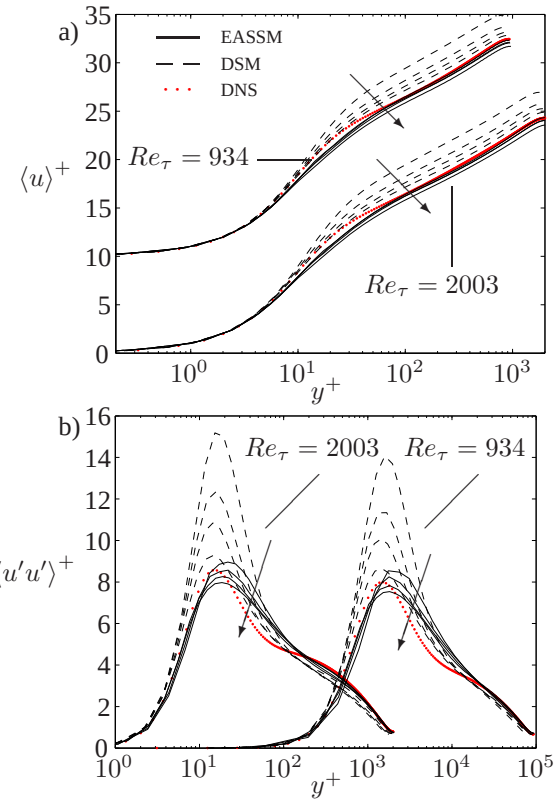

Figure 1: Mean velocity (a) and mean streamwise Reynolds stress (b) in wall units. Arrows point in the direction of increasing resolution.

4 Channel flow simulations at $Re_\tau = 934$ and 2003

Mean velocity profiles are shown in figure 1 (a). The DSM over-predicts the mean velocity profile at all resolutions indicating that the wall shear stress is under-predicted by this model, see also the Re_τ predictions in table 1. The EASSM predictions are close to the DNS profile at all resolutions and show a small dependence on the resolution and are more accurate than those of the DSM.

The streamwise Reynolds stresses are shown in figure 1 (b). At coarse resolutions the DSM largely over-predicts the Reynolds stress. This is a common behavior for isotropic eddy viscosity models at coarse resolutions (Rasam *et al.* 2011). The DSM results approach the DNS with increasing resolution. The EASSM predictions are close to the DNS profile and show a small dependence on resolution.

5 Part II: A new explicit algebraic subgrid scalar flux model (EASSFM)

The EASSFM is derived from the transport equation of the SGS scalar flux vector, q_i, i.e.

$$\frac{Dq_i}{Dt}=P^{\text{SGS}}_{i\theta}+D^{\text{SGS}}_{i\theta}+\Pi^{\text{SGS}}_{i\theta}-\epsilon^{\text{SGS}}_{i\theta}, \quad (6)$$

where $P^{\text{SGS}}_{i\theta}$ is the production, $D^{\text{SGS}}_{i\theta}$ includes turbulent and molecular diffusion, $\Pi^{\text{SGS}}_{i\theta}$ is the subgrid pressure

scalar-gradient correlation and $\epsilon_{i\theta}^{\rm SGS}$ is the molecular dissipation of q_i. We normalize q_i with the SGS kinetic energy, $K^{\rm SGS}$, and SGS scalar intensity, $K_\theta^{\rm SGS}$,

$$\xi_i = q_i/\sqrt{K^{\rm SGS}K_\theta^{\rm SGS}},$$
$$K^{\rm SGS} = \frac{1}{2}\left(\widetilde{u_i u_i} - \widetilde{u}_i\widetilde{u}_i\right), K_\theta^{\rm SGS} = \frac{1}{2}\left(\widetilde{\theta\theta} - \widetilde{\theta}\,\widetilde{\theta}\right). \quad (7)$$

The transport equation for ξ_i becomes

$$\frac{D\xi_i}{Dt} - D_i^\xi = -\frac{\xi_i}{2}\left(\frac{P_\theta^{\rm SGS} - \epsilon_\theta^{\rm SGS}}{K_\theta^{\rm SGS}} + \frac{P_K^{\rm SGS} - \epsilon_K^{\rm SGS}}{K^{\rm SGS}}\right) + \frac{P_{i\theta}^{\rm SGS} - \epsilon_{i\theta}^{\rm SGS} + \Pi_{i\theta}^{\rm SGS}}{\sqrt{(K^{\rm SGS}K_\theta^{\rm SGS})}}, \quad (8)$$

where $P_K^{\rm SGS}$ and $\epsilon_K^{\rm SGS}$ are the production and the dissipation of $K^{\rm SGS}$, respectively. $P_\theta^{\rm SGS}$ and $\epsilon_\theta^{\rm SGS}$ are the production and the dissipation of $K_\theta^{\rm SGS}$, respectively, and D_i^ξ is the diffusion of ξ_i. Following Wikström *et al.* (2000), we use the weak equilibrium assumption for ξ_i, i.e.

$$\frac{D\xi_i}{Dt} - D_i^\xi = 0\,. \quad (9)$$

We model $\Pi_{i\theta}^{\rm SGS} - \epsilon_{i\theta}^{\rm SGS}$, using the model employed by Wikström *et al.* (2000) and rewrite it in terms of q_i, τ_{ij} and filtered gradients instead of Reynolds averaged correlations and mean gradients,

$$\Pi_{i\theta}^{\rm SGS} - \epsilon_{i\theta}^{\rm SGS} = -c_{1\theta}q_i\frac{\epsilon_K^{\rm SGS}}{K^{\rm SGS}} + c_{2\theta}q_j\frac{\partial\widetilde{u}_i}{\partial x_j} + c_{3\theta}q_j\frac{\partial\widetilde{u}_j}{\partial x_i} + c_{4\theta}\tau_{ij}\frac{\partial\widetilde{\theta}}{\partial x_j}, \quad (10)$$

We further use the following equilibrium assumptions

$$P_\theta^{\rm SGS} = \epsilon_\theta^{\rm SGS}, \quad P_K^{\rm SGS} = \epsilon_K^{\rm SGS}, \quad (11)$$

to simplify the formulation. Using the model (10), the weak equilibrium assumption (9) and the equilibrium assumptions (11), equation (8) simplifies to a linear system of equations for q_j, i.e.

$$A_{ij}q_j = -(1-c_{4\theta})\tau^*\tau_{ij}\frac{\partial\widetilde{\theta}}{\partial x_j}, \quad (12)$$

where

$$A_{ij} = c_{1\theta}\delta_{ij} + c_S\widetilde{S}_{ij}^* + c_\Omega\widetilde{\Omega}_{ij}^*, \quad (13)$$

τ_{jk} is the SGS stress tensor, $\tau^* = K^{\rm SGS}/\epsilon_K^{\rm SGS}$ is the time scale of the subgrid velocity field, $c_S = (1 - c_{2\theta} - c_{3\theta})$ and $c_\Omega = (1 - c_{2\theta} + c_{3\theta})$. We use model (4) for τ^*. The normalized filtered strain rate and rotation-rate tensors are

$$\widetilde{S}_{ij}^* = \frac{\tau^*}{2}\left(\frac{\partial\widetilde{u}_i}{\partial x_j} + \frac{\partial\widetilde{u}_j}{\partial x_i}\right), \widetilde{\Omega}_{ij}^* = \frac{\tau^*}{2}\left(\frac{\partial\widetilde{u}_i}{\partial x_j} - \frac{\partial\widetilde{u}_j}{\partial x_i}\right).$$

We invert A_{ij} in (12) and obtain the EASSFM

$$q_i = -(1-c_{4\theta})\tau^* A_{ij}^{-1}\tau_{jk}\frac{\partial\tilde{\theta}}{\partial x_k} \quad (14)$$

where A_{ij}^{-1} is (bold face denotes tensor)

$$\begin{aligned}\mathbf{A}^{-1} =& \frac{(c_{1\theta}^2 - \frac{1}{2}Q_1)}{c_{1\theta}\left(c_{1\theta}^2 - \frac{1}{2}Q_1\right) + \frac{1}{2}Q_2}\mathbf{I} \\ &- \frac{c_{1\theta}}{c_{1\theta}\left(c_{1\theta}^2 - \frac{1}{2}Q_1\right) + \frac{1}{2}Q_2}(c_s\widetilde{\mathbf{S}}^* + c_\Omega\widetilde{\mathbf{\Omega}}^*) \\ &+ \frac{1}{c_{1\theta}\left(c_{1\theta}^2 - \frac{1}{2}Q_1\right) + \frac{1}{2}Q_2}(c_s\widetilde{\mathbf{S}}^* + c_\Omega\widetilde{\mathbf{\Omega}}^*)^2\,, \\ Q_1 =& \; c_s^2 tr(\widetilde{\mathbf{S}}^{*\mathbf{2}}) + c_\Omega^2 tr(\widetilde{\mathbf{\Omega}}^{*2}), \\ Q_2 =& \; \frac{2}{3}c_s^3 tr(\widetilde{\mathbf{S}}^{*3}) + 2c_s c_\Omega^2 tr(\widetilde{\mathbf{S}}^*\widetilde{\mathbf{\Omega}}^{*\mathbf{2}})\,, \end{aligned} \quad (15)$$

where $tr(.)$ denotes the trace of a matrix.

In the model (10), there are four parameters $c_{1-4\theta}$ that need to be prescribed. $c_{1\theta}$ is used in the model based on the return to isotropy concept of Rotta and models the small-scale interactions. In order to make $c_{1\theta}$ filter-scale independent we model that in terms of K^{SGS}, Δ, $|\tilde{S}_{ij}|$ and the SGS time scale of the scalar field, τ_θ, as

$$c_{1\theta} = c'_{1\theta}\left[\frac{K^{SGS}}{(0.1\Delta|\tilde{S}_{ij}|)^2}\right]\left(\tau_\theta|\tilde{S}_{ij}|\right)^{0.7}, c'_{1\theta} = 0.2, \quad (16)$$

where $\tau_\theta = Pr(\,K^{SGS}/\epsilon_k^{SGS})$ and Δ is the grid scale. Furthermore, to take into account the dependence of $c'_{1\theta}$ on the filter size and improve the predictions, we use the following correction

$$c'_{1\theta}(2\Delta) = 10^{-x}c'_{1\theta}(\Delta), x = 0.1\left(Re_{2\Delta}^{0.7} - Re_\Delta^{0.7}\right) - 0.3,$$

where $Re_{n\Delta} = n\Delta|\widetilde{S}_{ij}|/\nu$ is the mesh Reynolds number. This correction is an analytical power-law fit and is calibrated using *a priori* analysis of DNS data.

$c_{4\theta}$ is computed dynamically using the Germano identity for q_i in equation (14) using a test-filter with a size of 2Δ.

The effect of the model parameters c_Ω and c_s is similar to that of the $c_{4\theta}$ coefficient. Their values are found from *a posteriori* LES computations for the case of turbulent channel flow to be $c_\Omega = 0.5$ and $c_s = 0.2$.

Dynamic eddy diffusivity model (DEDM)

The performance of the EASSFM is compared to that of the DEDM, where the SGS scalar flux vector is modeled to be proportional to the large-scale gradient of the scalar

$$q_i = -\frac{\nu^{\rm SGS}(\Delta)}{Pr^{\rm SGS}}\frac{\partial\widetilde{\theta}}{\partial x_i}, \; \nu^{\rm SGS}(\Delta) = C_{\rm Smag}\Delta^2|\widetilde{S}_{ij}|, \quad (17)$$

where the SGS Prandtl number, $Pr^{\rm SGS}$, and the coefficient $C_{\rm Smag}$ for the computation of the SGS viscosity, $\nu^{\rm SGS}$, are computed dynamically using the Germano identity. Averaging of $C_{\rm Smag}$ and $Pr^{\rm SGS}$ in the homogeneous directions and clipping to positive values are done to stabilize the simulations.

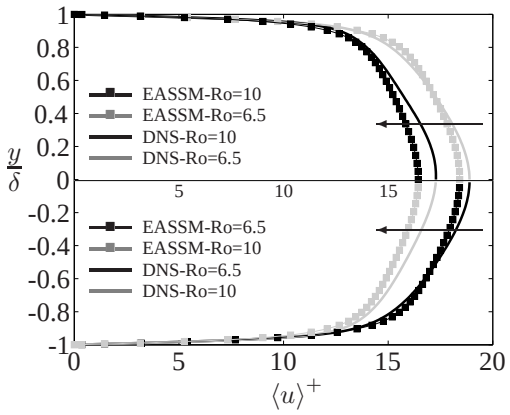

Figure 2: Mean streamwise velocity profiles in wall units. Note the different legends in the upper and lower halves of the figure. Arrows point in the direction of increasing rotation rate.

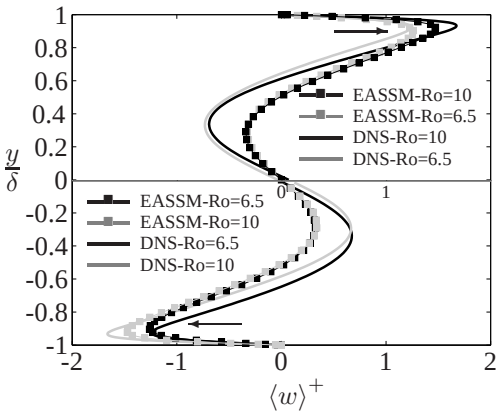

Figure 3: Mean spanwise velocity profiles in wall units. Note the different legends in the upper and lower halves of the figure. Arrows point in the direction of increasing rotation rate.

6 Channel flow simulations with streamwise system rotation and heat transfer

To evaluate the new EASSFM, we perform LESs and DNSs of turbulent channel flow with streamwise system rotation and heat transfer. The simulation parameters are given in table 2. The domain sizes and rotation rates are similar to those of the DNSs performed by Oberlack *et al.* (2006) at $Re_\tau = 180$, without heat transfer. The DNSs and LESs are carried out at $Re_\tau = 300$ using a constant pressure gradient constraint. Channel walls are kept at constant but different temperatures and the Prandtl number is $Pr = 0.71$. The rotation numbers shown in table 2 are expressed in wall units, i.e. $Ro^+ = \delta\Omega/u_\tau$, where u_τ is the friction velocity. The EASSM is used in all LESs. LES

Case	Ro^+	Δx^+	Δz^+	N_y	$\frac{L_x}{\delta}$	$\frac{L_z}{\delta}$	SGS scalar-flux model	Nusselt Number
1	6.5	39.3	19.6	65	4π	2π	EASSFM	5.77
							DEDM	5.63
2	10.0	39.3	19.6	65	8π	4π	EASSFM	6.93
							DEDM	6.78
3	6.5	14.7	7.4	193	4π	2π	–	5.72
4	10.0	14.7	7.4	193	8π	4π	–	6.97

Table 2: Summary of the simulations. L_x, L_z and 2δ are the domain sizes in the streamwise, spanwise and wall-normal directions, respectively. Cases 3-4 are DNSs.

results using the EASSFM are compared to those of the DNS and the DEDM.

Mean velocity profiles

Figures 2 and 3 show LES and DNS predictions of the mean streamwise and spanwise velocity profiles, respectively, in wall units. Rotation reduces the mean streamwise velocity, while it induces a mean spanwise velocity with a skew-symmetric profile.

LES prediction of the mean streamwise velocity at the lower rotation rate (case 1) is in better agreement with the DNS (case 3) than the one at the higher rotation rate (case 2). The LES predictions of the mean streamwise velocity profiles are flatter than those of the DNS in the core of the channel. The spanwise velocity profiles are satisfactorily predicted by the LES in the near-wall region, while in the core of the channel the predictions are not as good.

Mean and RMS profiles of temperature

Figure 4(a) shows the mean temperature profiles in wall units. Rotation sharpens the temperature gradient in the diffusion-dominated near-wall region ($y^+ Pr < 10$) and therefore enhances the heat transfer and mixing in the near-wall region. It decreases the slope of the mean temperature in the core of the channel indicating a reduction of the production in that area. The EASSFM predictions are slightly better than those of the DEDM.

The root-mean-square (RMS) of the temperature fluctuations is shown in figure 4(b). The RMS profiles have two peaks. The near-wall peak corresponds to the location of the maxima in the production of the scalar variance. The outer peak is due to the non-zero production due to the temperature gradient in the core of the channel. The former becomes larger with increasing rotation, since the production of the scalar variance increases with rotation, and the latter becomes weaker with increasing rotation due to the decrease in the temperature gradient in the core of the channel.

The EASSFM predictions are better than those of the DEDM in the near-wall region, while the DEDM predictions are better in the core of the cannel.

Resolved heat fluxes

Figure 5(a) shows the mean streamwise heat fluxes for the DNS and the corresponding resolved plus modeled heat fluxes from the LES in wall units at different rotation rotes. The streamwise heat flux decreases with increasing rotation rate. The LES predictions are in

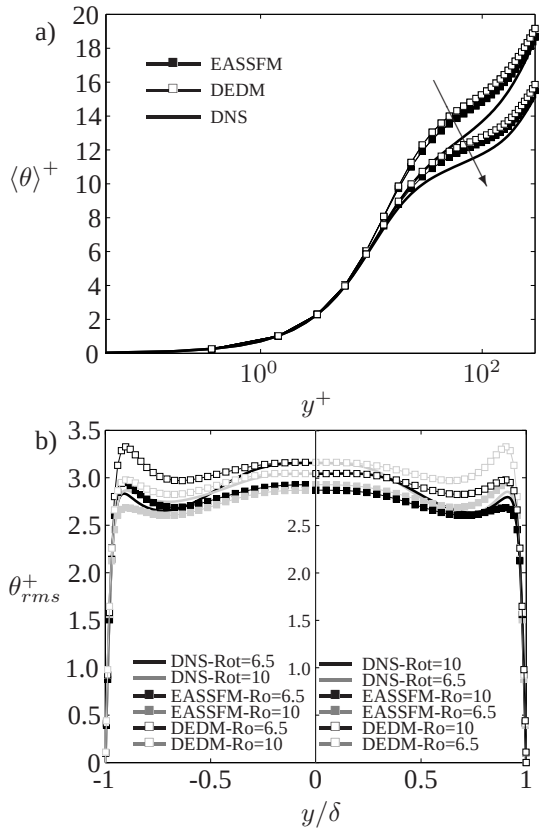

Figure 4: Mean temperature profiles (a) and root-mean-square (RMS) profiles of the temperature (b) in wall units. Note the different legends in the left and right halves of figure (b). Arrow in figure (a) points in the direction of increasing rotation rate.

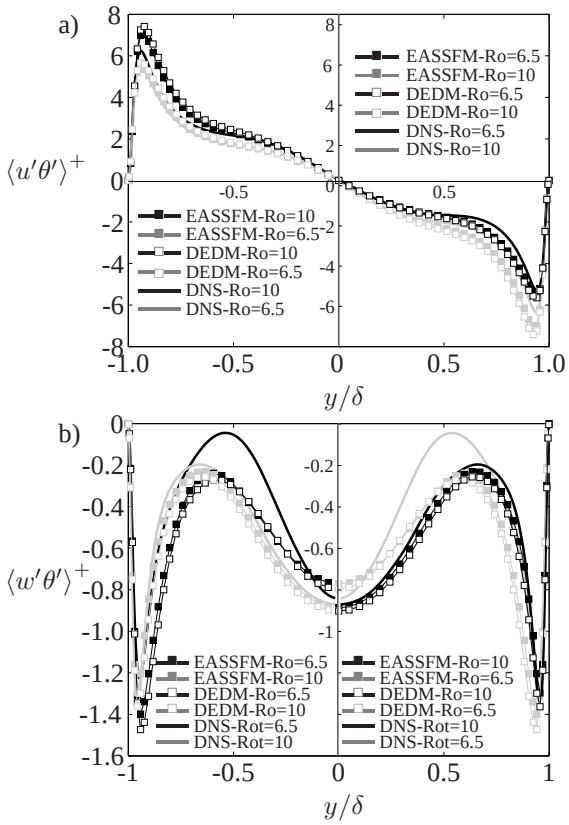

Figure 5: Resolved plus modeled mean streamwise (a) and spanwise (b) heat fluxes in wall units. Note the different legends in the left and right halves of the figures.

good agreement with the DNS and the differences are small between the two model predictions at these resolutions. The EASSFM predictions are slightly better than those of the DEDM.

Rotation creates a mean spanwise heat flux which is symmetric about the channel center line and increases with increasing rotation rate, see figure 5(b). The LES predictions are in better agreement with the DNS at the higher rotation rate (case 2). The EASSFM predictions are slightly better than those of the DEDM at both rotation rates.

It has to be noted that all the SGS heat fluxes are nonzero in the spanwise rotating channel flow. The DEDM predicts zero streamwise and spanwise SGS heat fluxes, while the EASSFM predictions are in good agreement with the filtered DNS data (results are not shown here).

Near-wall turbulent structures

Visualizations of instantaneous streamwise and spanwise velocity and temperature fluctuations at $y^+ \approx 15$ are shown in figures 6-8. The streamwise velocity fluctuations show streaky structures which are characteristics of wall-bounded flows. Due to rotation, the structures are tilted towards the spanwise direction. The structures predicted by the LES are both wider and longer than those of the DNS. The spanwise velocity fluctuations show patterns of high and low intensities which are not similar to those of the streamwise velocity fluctuations but are also tilted to the spanwise direction, see figures 7(a-b). The temperature fluctuations show streaky structures similar to those of the streamwise velocity fluctuations, see figures 8(a-b).

7 Conclusions

We presented channel flow LES results using the explicit algebraic subgrid stress model (EASSM) of Marstorp *et al.* (2009) at $Re_\tau = 934$ and 2003 and various resolutions. The EASSM predictions were compared to LES predictions using the dynamic Smagorinsky model (DSM) of Germano *et al.* (1991) and DNS data. The EASSM takes into account the anisotropy of the SGS in its formulation through nonlinear terms involving the strain rate and rotation-rate tensors. As a consequence of its better formulation, the EASSM predictions were shown to be less resolution dependent than the ones of the DSM, regarding the mean velocity and Reynolds stresses, and its predictions were much more accurate at coarse resolutions. Therefore, the EASSM can produce LES predictions with the same accuracy as the DSM but at a lower resolution

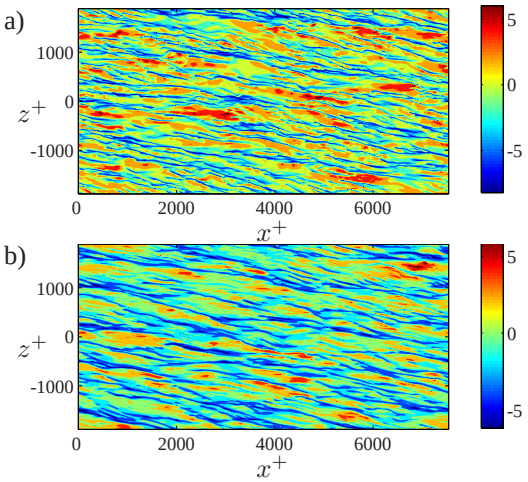

Figure 6: Instantaneous streamwise velocity fluctuations from DNS (case 4) (a) and LES (case 2) (b) at $y^+ \approx 15$.

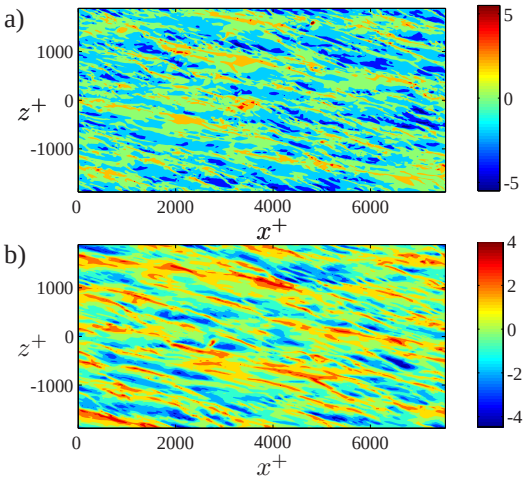

Figure 7: Instantaneous spanwise velocity fluctuations from DNS (case 4) (a) and LES (case 2) (b) at $y^+ \approx 15$.

and therefore a much lower computational cost.

In analogy with the EASSM, we derived an explicit algebraic subgrid scalar flux model (EASSFM) from the explicit algebraic model of Wikström *et al.* (2000) for the Reynolds averaged scalar transport equations. Contrary to the dynamic eddy diffusivity model (DEDM), the new model predictions are not aligned with the resolved scalar gradients. Therefore, it can predict SGS fluxes induced by the mean shear. To test the new EASSFM, we performed LES of channel flow at $Re_\tau = 300$ with heat transfer and streamwise rotation for two rotation rates. The EASSFM improved the predictions of the mean temperature and the resolved heat fluxes over the DEDM.

Acknowledgments

This work was supported by the Swedish Research Council through grant number 621-2010-6965. Funding from *Erik Petersohns Minne* and the computer time provided by the Swedish National Infrastructure for Computing (SNIC) are gratefully acknowledged.

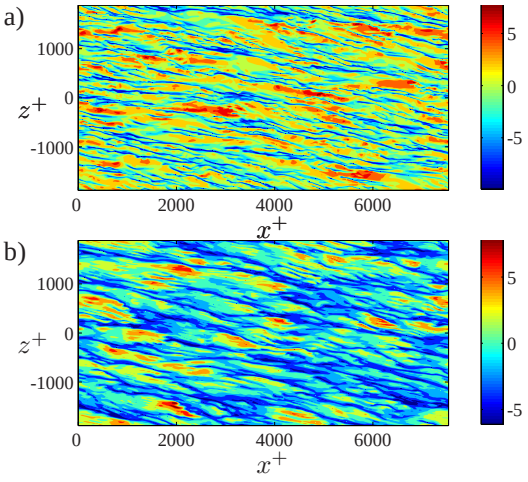

Figure 8: Instantaneous temperature fluctuations from DNS (case 4) (a) and LES (case 2) (b) at $y^+ \approx 15$.

References

Chevalier, M., Schlatter, P., Lundbladh, A. and Henningson, D. S. (2007), SIMSON a pseudo-spectral solver for incompressible boundary layer flows. *Tech. Rep. 2007:07*. KTH Mechanics, SE-10044 Stockholm, Sweden.

Germano, M., Piomelli, U., Moin P. and Cabot, W. H. (1991), A dynamic subgrid-scale eddy viscosity model. *Phys. of Fluids A*, Vol. 3(7), pp. 1760-1765.

Hoyas, S. and Jiménez, J. (2008), Reynolds number effects on the Reynolds-stress budgets in turbulent channels. *Phys. of Fluids*, Vol. 20, 101511.

Kang, H. S. and Meneveau C. (2001), Passive scalar anisotropy in a heated turbulent wake: new observations and implications for large eddy simulations. *J. Fluid Mech.* Vol. 442, pp. 161-170.

Marstorp, L., Brethouwer, G., Grundestam O. and Johansson, A.V. (2009), Explicit algebraic subgrid stress models with application to rotating channel flow *J. Fluid Mech.*, Vol. 639, pp. 403-432.

Moin, P., Squires, K., Cabot, W. and Lee, S. (1991), A dynamic subgrid-scale model for compressible turbulence and scalar transport *Phys. of Fluids A*, Vol. 3, pp. 2746-2757.

Oberlack, M., Cabot, W., Pettersson Reif, B. A. and Weller T. (2006), Group analysis, direct numerical simulation and modelling of a turbulent channel flow with streamwise rotation. *J. Fluid Mech.*, Vol. 562, pp.383-403.

Rasam A., Brethouwer G., Schlatter P., Li Q. and Johansson A. V. (2011), Effects of modelling, resolution and anisotropy of subgrid-scales on large eddy simulations of channel flow. *J. Turbulence*, Vol. 12(10), pp. 1-20.

Rodi, W. (1976), A new algebraic relation for calculating the Reynolds stresses. *Z. Anew. Math. Mech.*, Vol. 56, T219.

Sagaut, P. (2010.) Large Eddy Simulation for Incompressible Flows: An Introduction. *3rd Edition Springer*.

Wallin, S. and Johansson, A. V. (2000), An explicit algebraic Reynolds stress model for incompressible and compressible turbulent flows *J. Fluid Mech.*, Vol. 403, pp.89-132.

Wikström, P. M., Wallin, S. and Johansson, A.V. (2000), Derivation and investigation of a new explicit algebraic model for the passive scalar flux *Phys. Fluids*, Vol. 12(3), pp. 688-702.